






Article

# Hardware Prototyping and Validation of a W- $\Delta$ DOR Digital Signal Processor

Gian Carlo Cardarilli <sup>1,\*</sup>, Luca Di Nunzio <sup>1,\*</sup>, Rocco Fazzolari <sup>1,\*</sup>, Daniele Giardino <sup>1</sup>,  
Marco Matta <sup>1,\*</sup>, Marco Re <sup>1</sup>, Luciano Iess <sup>2</sup>, Fabio Cialfi <sup>3</sup>, Giorgio De Angelis <sup>3</sup>,  
Dario Gelfusa <sup>3</sup>, Ascanio Patrizio Pulcinelli <sup>3</sup> and Lorenzo Simone <sup>3</sup>

<sup>1</sup> Department of Electronic Engineering, University of Rome Tor Vergata, 00133 Roma, Italy

<sup>2</sup> Department of Mechanical and Aerospace Engineering, University of Rome La Sapienza, 00184 Roma, Italy

<sup>3</sup> Thales Alenia Space Italia, Via Saccomuro, 24, 00131 Roma RM, Italy

\* Correspondence: cardarilli@ing.uniroma2.it (G.C.C.); di.nunzio@ing.uniroma2.it (L.D.N.); fazzolari@ing.uniroma2.it (R.F.); matta@ing.uniroma2.it (M.M.); Tel.: +39-06-7259-7810 (L.D.N.)

Received: 21 June 2019; Accepted: 18 July 2019; Published: 20 July 2019



**Abstract:** Microwave tracking, usually performed by on ground processing of the signals coming from a spacecraft, represents a crucial aspect in every deep-space mission. Various noise sources, including receiver noise, affect these signals, limiting the accuracy of the radiometric measurements obtained from the radio link. There are several methods used for spacecraft tracking, including the Delta-Differential One-Way Ranging ( $\Delta$ DOR) technique. In the past years, European Space Agency (ESA) missions relied on a narrowband  $\Delta$ DOR system for navigation in the cruise phase. To limit the adverse effect of nonlinearities in the receiving chain, an innovative wideband approach to  $\Delta$ DOR measurements has recently been proposed. This work presents the hardware implementation of a new version of the ESA X/Ka Deep Space Transponder based on the new tracking technique named Wideband  $\Delta$ DOR (W- $\Delta$ DOR). The architecture of the new transponder guarantees backward compatibility with narrowband  $\Delta$ DOR.

**Keywords:**  $\Delta$ DOR; W- $\Delta$ DOR; spacecraft tracking

## 1. Introduction

This paper presents the hardware implementation and characterization of a novel Delta-Differential One-Way Ranging ( $\Delta$ DOR) technique based on spread-spectrum waveforms [1,2]. The relative angular position of a spacecraft with respect to known radio sources (typically, quasars) is currently determined by means of differential phase measurements using Very Long Baseline Interferometry (VLBI) technique [3,4] according to CCSDS 500.1-G-1 *Delta-DOR Technical Characteristics and Performance*. In practice, the difference in arrival times of spacecraft radio signals at two widely separated ground stations is accurately measured, along with similar differential phase measurements of a nearby quasar. The quasar, being one of the radio sources defining the International Celestial Reference Frame (ICRF), has known angular coordinates and can serve as a fiducial landmark to reference the spacecraft phase (Figure 1).

The spacecraft location is measured with excellent accuracy relative to the ICRF frame [5]. The ESA  $\Delta$ DOR system attains consistently angular accuracies of a few nanoradians (corresponding to delays in the order of  $10^{-10}$  s). Precise angular measurements are extremely valuable for both spacecraft navigation and scientific investigations of Solar System dynamics. The knowledge of the angular position proves very important, especially in the planetary approach phase in order to prepare and execute the planetary orbit insertion.

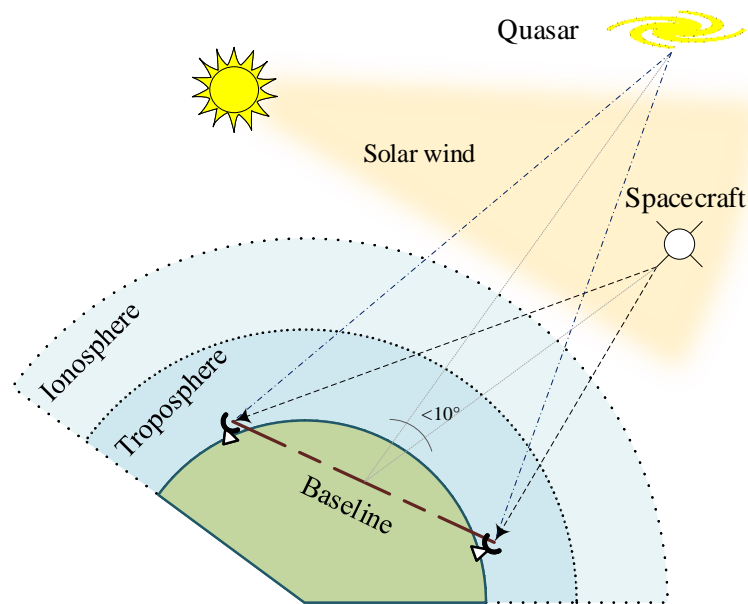


**Figure 1.**  $\Delta$ DOR measurement principle and geometry.

Although Doppler observables also provide angular information,  $\Delta$ DOR observations are intrinsically more accurate and less dependent on the dynamical model of the spacecraft [6,7]. The targeting of the capture maneuver (for an orbiter) or the Entry, Descent, and Landing (EDL) phase greatly benefit from, and even rely on, previous  $\Delta$ DOR observations. Accurate Solar System bodies and satellite ephemerides are crucial for Solar System exploration. In addition, the generation of precise ephemerides requires an accurate formulation of Solar System dynamics in the context of a fully relativistic model. Conversely, tracking the motion of Solar System bodies is an excellent experimental tool to test the adopted laws of gravity. The Solar System constitutes indeed the cleanest environment to carry out determinations of the space-time metric in the weak field limit, and to assess the range of validity of general relativity. The observable of choice for Solar System dynamics investigations are range and  $\Delta$ DOR. The two set of measurements complement each other, with  $\Delta$ DOR providing unique information in the out-of-plane components of planets and satellites positions. The orbits are determined by first referencing the orbit of the spacecraft to the planetary body using Doppler measurements, and then linking the body's position to a Solar System barycentric frame by means of angular and range measurements. Other interesting applications of interferometric techniques are related to the relative positioning of two spacecraft, landers, or a lander and an orbiter. This technique, called Same Beam Interferometry (SBI) [8], was originally proposed in a configuration with two antennas tracking simultaneously two probes in one-way mode.

However, SBI can be considered in a simpler configuration where a single ground antenna tracks, simultaneously in two-way mode, two probes separated by a small line-of-sight angle (0.5 degrees or less). This powerful method allows a considerable improvement in the positioning of a probe when the orbit (or the position) of the second one is well determined. The coherent downlink signals coming from each probe are combined to form the differential phase, proportional to the relative distance between each probe of the pair. In the case of two (or more) landers, SBI would provide very accurate measurements of tides and rotational state of a planetary body, which are used in geophysical models to constrain the interior structure and evolution.

The scenario where two landers are deployed on the surface of Mars is particularly interesting since differential range accuracies of the order of 1–10 mm can be attained. SBI measurements to

a network of landers on the moon would provide differential range at least an order of magnitude more precise, thus providing useful geophysical information on the lunar interior.

This level of accuracy can be obtained by means of two-way radio links in X or Ka band enabled by suitably designed digital transponders and spread spectrum radio links, as described in this paper. Spread spectrum signals not only allow a reduction of the differential group delays in  $\Delta$ DOR and SBI measurements, but also enable simultaneous communications to multiple spacecraft from a single antenna, a scenario that is already occurring at Mars. The spacecraft group-delay measures involve differencing the measured phase of two or more discrete tones transmitted by the spacecraft. The measured phase difference between a pair of tones, divided by their frequency separation, is the primary group-delay observable. This is in contrast to the several-MHz bandpass used to measure the quasar group delays, therefore a systematic error is induced in the  $\Delta$ DOR measure, as outlined in Figure 2.

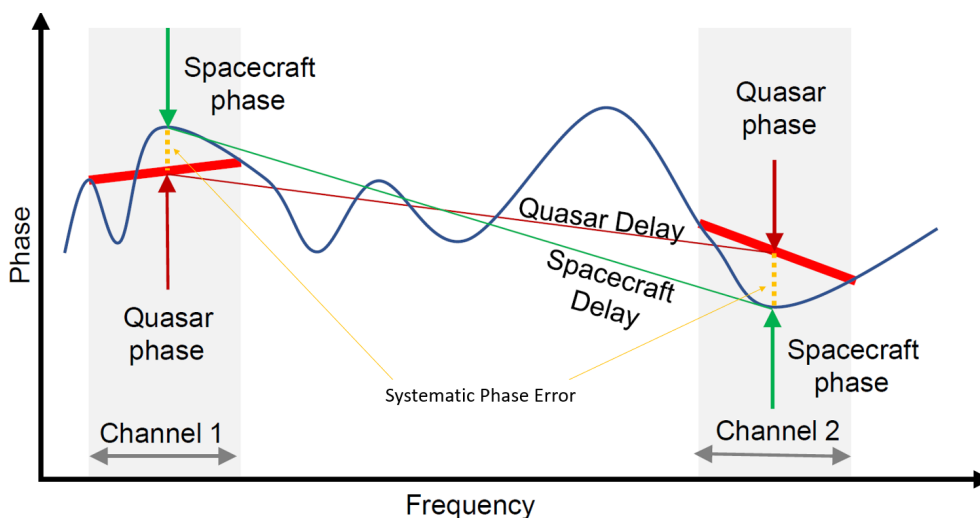


Figure 2. Systematic error in  $\Delta$ DOR measurements.

The blue curve shows the phase dispersion as a function of frequency, while the green line shows the average linear behavior. At the spacecraft tone frequency (arrows), the measured phase differs between the narrowband spacecraft measurement (green) and the wideband quasar measurement (red), resulting in systematic phase error. To minimize the systematic error, the on-board synthesized  $\Delta$ DOR signal should resemble the quasar one as much as possible [9]. Thanks to the differential nature of the measurement, the difference between the spacecraft and quasar delays produces an observable that minimizes calibration errors due to instrument dispersion, especially the ones due to phase ripples in the acquisition filter, thus providing enhanced performances [10]. The recent advancements in the field of on-board microelectronics, e.g., Digital Signal Processing cores for space applications, are enabling factors to develop the newest  $\Delta$ DOR paradigm based on broadband observables: Wideband  $\Delta$ DOR.

## 2. Thales Alenia Space Transponder Platform

The core of the novel Wideband  $\Delta$ DOR (W- $\Delta$ DOR) will be integrated in the new Thales Alenia Space (TAS) Transponder Platform based on the TAS deep-space transponder architecture and depicted in Figure 3.

This transponder has been conceived as a common platform, composed of common blocks coupled with custom parts. The common platform includes: the Digital Section (ASIC, FPGA, DACs, ADC), the Transmitter Radio Frequency (RF)/Intermediate Frequency (IF) section and the Receiver RF/IF section. The custom parts include: the DC/DC Converters, the Programmable Read-Only Memory (PROM) Interface, the RF Front-End and Back-End sections and the Interface Card. The platform approach allows the TAS transponder to be very flexible and reconfigurable

in terms of physical modules and mapped cores on the internal FPGA. Different missions will require different sets of DC/DC Converters, programmable read-only memories, interfaces and RF front-end and back-end. Conversely, the transponder core, composed of the digital and RF/IF sections, will remain unchanged [11,12]. The new transponder named Flexible Autonomous Transponder (FAT) has been derived from the TAS transponder heritage regarding Deep-Space, Radio-Science, Near Earth and Secure Spread-Spectrum TT&C product lines. The different functions are implemented in the following modules:

- Dual Band Receiver Analogue Module
- Digital Module
- X-Band Transmitter Analogue Module
- Ka-Band Transmitter Module
- Baseplate Module

The FAT architecture has been conceived to support, by means of the same hardware, different mission scenarios and applications. For example, deep-space missions such as BepiColombo and JUICE feature regenerative ranging with low chip rate (3 Mcps) and radio science experiments with high chip rate regenerative ranging (24 Mcps) for accurate ranging measurements. The FAT digital core is conceived around the Ka-band Transponder (KaT) ASIC that fully supports all required modulation schemes and processing needs. The KaT ASIC has been developed in the frame of BepiColombo/MORE program, in which a new digital platform has been developed by TAS aiming to cover all TT&C modulation standards (spread-spectrum, FM, and PM) and mission profiles, from deep-space to near-Earth.

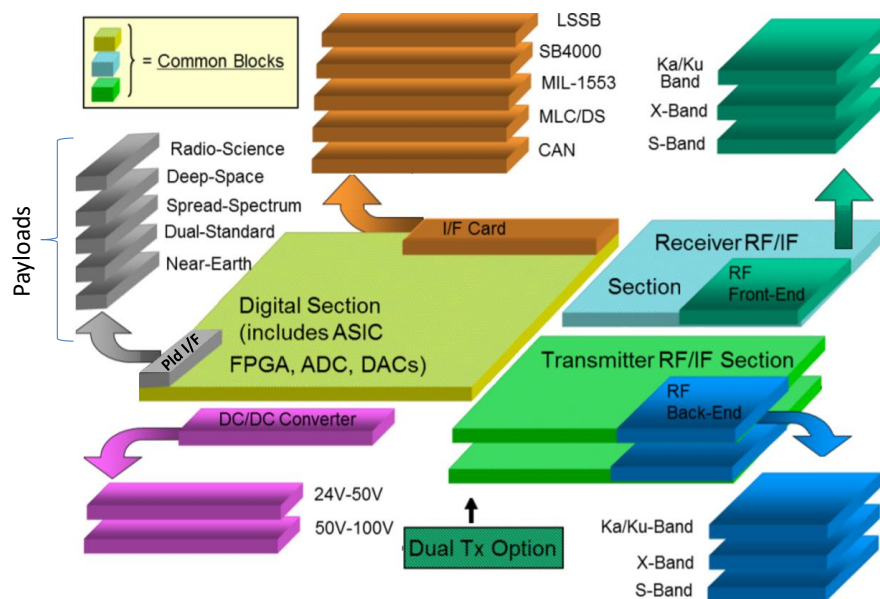


Figure 3. TAS-I transponder platform architecture.

Moreover, it includes a powerful microprocessor, i.e., the LEON2-FT [13], implementing the first System-on-Chip (SoC) devoted to on-board TT&C missions. Through the AMBA bus, the LEON2-FT is able to configure and control the different DSP functional blocks such as: carrier processing (that receives samples from the ADC), telecommand processing, ranging channels, telemetry block (that receives telemetry data from the on-board computer for down-link modulation), DDS parameters and functions for the Rx and Tx blocks. Moreover, through the memory bus, the KaT embedded microprocessor can access external devices for configuration and control. In particular, the LEON2-FT can access the FPGA where the novel  $W-\Delta$ DOR core is loaded.

### 3. W-ΔDOR Hardware Implementation

This section provides a description of the W-ΔDOR DSP core hardware implementation. The down-link (DL) signal is Equation (1).

$$s_{DL}(t) = A \sin [2\pi f_c t + TC(t) + s_{W\Delta DOR}(t)] \quad (1)$$

It is the modulation of a X/Ka-band carrier by means of pseudo-noise phase components. In Equation (1),  $A$  represents the signal amplitude,  $f_c$  is the X- or Ka-band carrier frequency,  $TC(t)$  represents telemetry and command signals and  $s_{W\Delta DOR}$  is the spread spectrum component of the W-ΔDOR signal. This method is proposed in [1] with the purpose of compatibility with the BepiColombo X/Ka Deep-Space Transponder design [11]. The signal represented in W-ΔDOR part is the summation of  $N$  sub-carriers of frequency  $f_i$ .

$$s_{W\Delta DOR}(t) = \sum_{i=1}^N \phi_i PN_i \sin(2\pi f_i t) \quad (2)$$

They are modulated by pseudo-random noise sequences  $PN_i$  of amplitude  $\phi_i$ .

#### 3.1. W-ΔDOR DSP Core Architecture Description

The W-ΔDOR DSP core is implemented in the FPGA available in the transponder digital section and generates the signal defined by Equation (2). Detailed system specifications are provided in [1]. The system clock frequency is  $8F1 = 76.8$  MHz where  $F1$  is 9.6 MHz for compatibility with the work in [1,11]. The main technical specifications are:

- Selectable chip rates:  $\frac{F1}{2}$ ,  $\frac{F1}{3}$ ,  $\frac{F1}{4}$  and  $\frac{F1}{8}$  for tuning the spectrum width of the DOR observables;
- Selectable sub-carrier tones:  $\frac{F1}{2}$  and  $2F1$ , for the spectrum allocation of the observables;
- Complete in-flight parameters reprogrammability; and
- Backward compatibility with narrowband ΔDOR.

The LEON2-FT microprocessor is in charge to enable/disable the core. Moreover, the LEON2-FT can read and write the W-ΔDOR core parameters by using a register file internal to the FPGA. These registers contain different parameters such as chip rates and sub-carriers frequency words. A control register is also included to enable and reset the W-ΔDOR core and to set up the narrowband compatibility mode. The on-chip communication occurs through a dedicated bus controlled by a custom IP core called LEON2-FT Interface Bus Controller. The W-ΔDOR core has two outputs: Root Raised-Cosine (RRC) and Non-Return-to-Zero (NRZ). The RRC output is interfaced with a 10-bit D/A converter connected to both the X and Ka transmission modules, while the NRZ signal feeds the Ka transmission module. The architecture of the core is detailed in Figure 4; it consists of two sub-parts, named *RRC Section* and *NRZ Section*.

The proposed W-ΔDOR core has been designed for  $N = 3$  with reference to Equation (2), with one NRZ- and two RRC-shaped signal components. Hence, the RRC and NRZ sections have, respectively, two and one data paths. A detailed description of the W-ΔDOR core components is provided in the following subsections.

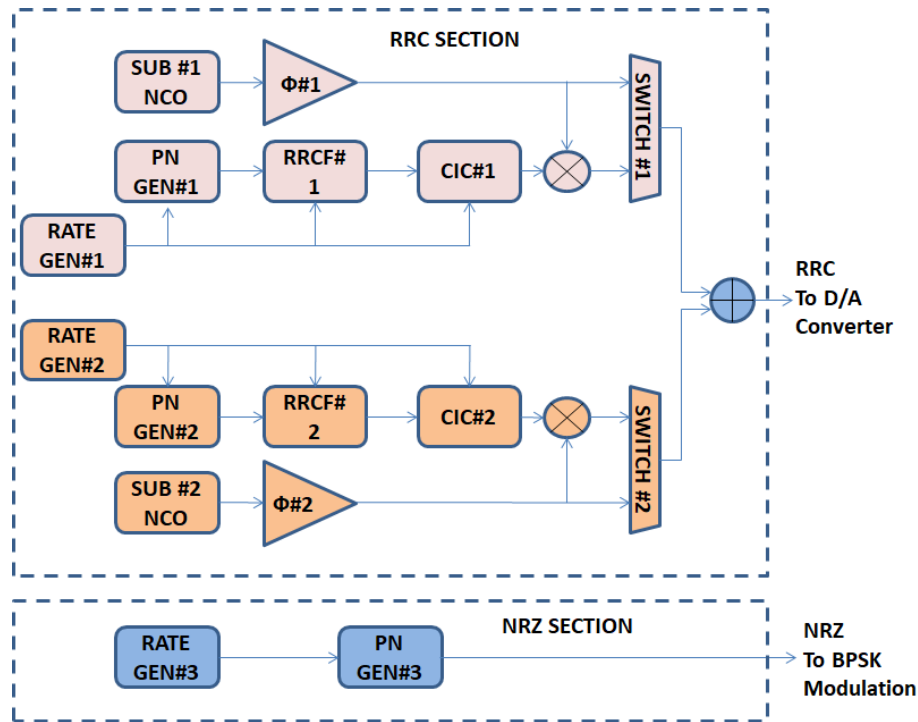


Figure 4. W- $\Delta$ DOR core DSP architecture.

### 3.1.1. Rate Generator

The different sampling rates and chip rates are derived from the main clock at frequency  $8F_1$ . The Rate Generator generates two enable signals: the first one is used by the PN generator to control the output chip rate, and the second one is used to tune the sampling rate of the output section of the RRC filter and the input section of the CIC filter.

### 3.1.2. Pseudo Noise Generator

A set of two Linear Feedback Shift Registers (LFSRs) generates the PN sequences. The output registers are combined to obtain a Gold Code. The seeds and the generating polynomials are reconfigurable.

### 3.1.3. Root Raised Cosine Shaping Filter (RRCF)

This filter interpolates and shapes the incoming PN code. The coefficients are reconfigurable, the filter order is 128 and the interpolation factor is 8. It is implemented in transposed form and the polyphase decomposition (eighth order) is applied for optimizing the computational load. The resulting 136 filter coefficients (129 plus 7 null padding values) are distributed in a total of 17 memories containing each of the eight phase coefficients. No multipliers are required as the input signal is single bit, i.e., it can assume only the values  $-1$  (coded as 0 logic) and  $1$  (coded as 1 logic). The multiplication of the 12-bit coefficients is performed by multiplexers, which select the current values or the additive inverse, computed by using a radix-2 complement converter.

### 3.1.4. CIC Interpolation Filter

The output of the RRC Filter needs further interpolation because the chip rate is parametric. The rate change is performed by using a Comb-Interpolation-Cascaded (CIC) filter that offers several advantages:

- The interpolation factor is easy to reconfigure with respect to other approaches.
- The algorithm does not require multipliers.



- It provides a linear phase response.

The implemented CIC filter is composed of four sections, obtaining a stop-band attenuation of 80 dB minimum. The Comb filter section registers are 12-bit wide, while the integration section registers width is 23 bit, as shown in [14]. The filter output word length is truncated to 16 bits.

### 3.1.5. Subcarrier Generation

The W- $\Delta$ DOR DSP core must generate two subcarriers at  $\frac{F_1}{2}$  and  $2F_1$ . Two Numeric Controlled Oscillators (NCOs) are used: the phase accumulator is 32-bit wide, while the phase is truncated to 16 bits. The phase-to-amplitude conversion is performed by a 14-iteration CORDIC. Each iteration is computed in parallel to maximize the throughput. The NCO output register is 16-bit wide. Additional blocks in the RRC section are: two switches for selecting the narrowband/wideband configuration, attenuators (named  $\phi\#$ ) to implement modulation indexes, multipliers to modulate the subcarriers, and an adder to mix the two waveforms.

### 3.2. Simulation and Synthesis Results

The W- $\Delta$ DOR DSP core was simulated in MATLAB & Simulink, in both floating point (FLP) and fixed point (FXP) arithmetic. A simulation-based FLP to FXP optimization flow was performed to minimize the registers word length maintaining the target specification of 50 dB of Dynamic Range on the generated RRC signal depending on the modulation index value. The W- $\Delta$ DOR core architecture (Figure 2) was coded in VHDL, synthesized by using ALTERA Quartus II 13 IDE Tool, and was implemented on an ALTERA Stratix II EP2S180 FPGA. The maximum clock frequency was 137.9 MHz (100 MHz required). A summary of the hardware resources usage (post Place & Route) is shown in Table 1.

**Table 1.** ALTERA Stratix II EP2S180 FPGA Resources utilization.

RESOURCES	USAGE	QUOTA
COMBINATIONAL ALUTS	5720/143250	4%
DEDICATED LOGIC REGISTERS	13488/143520	9%
ALMs: partially or completely used	9075/71760	13%
Total LABs:partially or completely used	1193/8970	9%
I/O PINS	79/743	11%

### 3.3. Experimental Results

The W- $\Delta$ DOR bread-board is composed of a 0.18  $\mu$ m ATMEL KaT ASIC (i.e., ATC18RHA family) integrated in the TAS digital transponder platform [12,15] and by an ALTERA FPGA Stratix II DSP development board implementing the W- $\Delta$ DOR core. The SRAM memories, integrated in the TAS digital transponder platform, are shared between the ATMEL KaT ASIC and the FPGA through a common address and data bus. The KaT ASIC includes the LEON2-FT microprocessor that is devoted to the W- $\Delta$ DOR core configuration and monitoring. The W- $\Delta$ DOR signals, converted in the analog domain by the FPGA development board DAC, were characterized using a Keysight PSA E4440 spectrum analyzer (the TAS experimental setup is shown in Figure 5).

The testbed is composed of:

- FAT Digital module
- RF module that includes the RX section plus the TX section
- Up-link signal generation and modulation that includes:
  - U/L signal generator
  - Subcarrier and data generators
  - BER meter

PM Modulator

Two counters

- Spectrum analyzer for spectral analysis
- Leon2FT debugger
- MIL-BUS-1553 Controller
- CNT90 counter for Allan deviation and frequency stability measurements
- FPGA Altera for W-ΔDOR signal generation
- Oscilloscope
- Power supplies for RF module
- STD Ranging generation and demodulation that includes:

Network analyzer

TASI PM demodulator

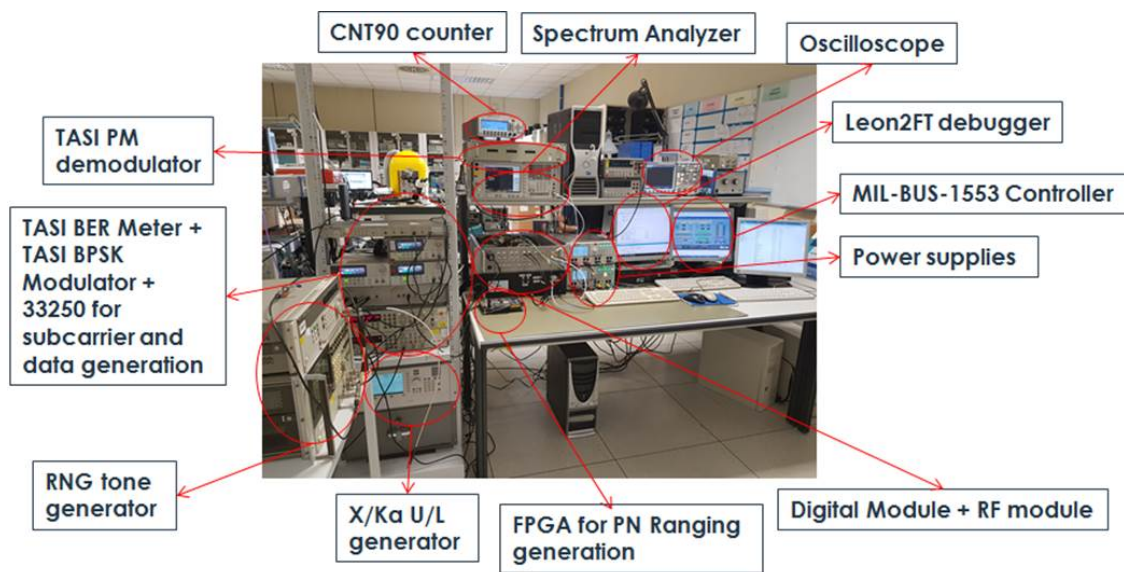


Figure 5. TAS W-ΔDOR experimental setup.

The experiments were performed on different test cases corresponding to different sets of the configuration, provided in Table 2.

Table 2. Test cases configuration parameters.

PARAM.	TEST 1	TEST 2	TEST 3	TEST 4	TEST 5
subc1 freq.	F1/2	F1/2	F1/2	F1/2	F1/3
subc2 freq.	2F1	2F1	2F1	2F1	3F1/2
ChipRate1	F1/2	F1/8	F1/8	F1/8	F1/3
ChipRate2	F1/2	F1/8	F1/4	F1/2	F1/3
ChipRate3	F1/2	F1/8	F1/2	F1/3	F1/3
$\phi_1$	1	0.5	0.25	0.125	0.125
$\phi_2$	1	0.5	1	0.125	1

The spectra obtained by simulation and from experimental measurements, illustrated in Figures 6 and 7 (Test Case 1) and in Figures 8 and 9 (Test Case 4), match well, excluding a gain bias due to the digital-to-analog conversion.

In particular, Figure 6 shows the measured output spectrum achieved with the subcarrier 1 at frequency F1/2 and subcarrier 2 at frequency 2F1, both modulated with the PN code at chip rate F1/2. In this case, the modulation index is set to 1 rad-pk. The DAC sampling frequency is about 76 MHz,



thus the Nyquist window from 0 to about 38 MHz is reported. In Figure 8, the measured output spectrum corresponding to Test Case 4 is reported. In this condition, the subcarrier 1 at frequency  $F1/2$  is modulated by a PN code at  $F1/8$ , while the subcarrier 2 at frequency  $2F1$  is modulated with PN code at rate  $F1/2$ . This test also shows the ability of the  $W-\Delta$ DOR to independently set the amplitude of each subcarrier.

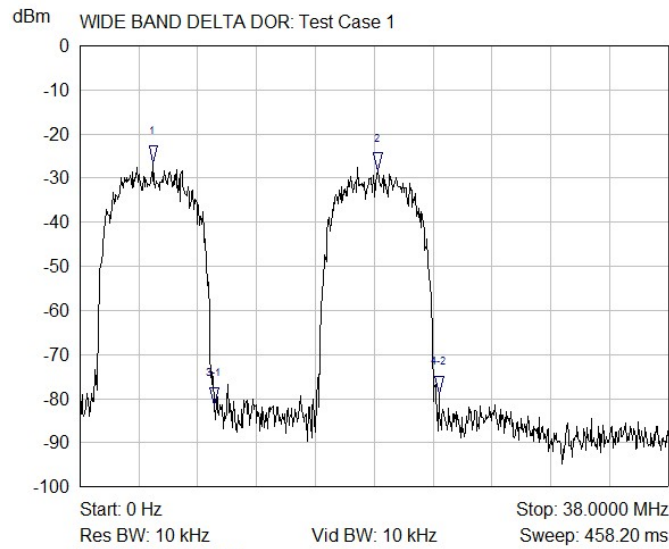


Figure 6. Test case 1 measured.

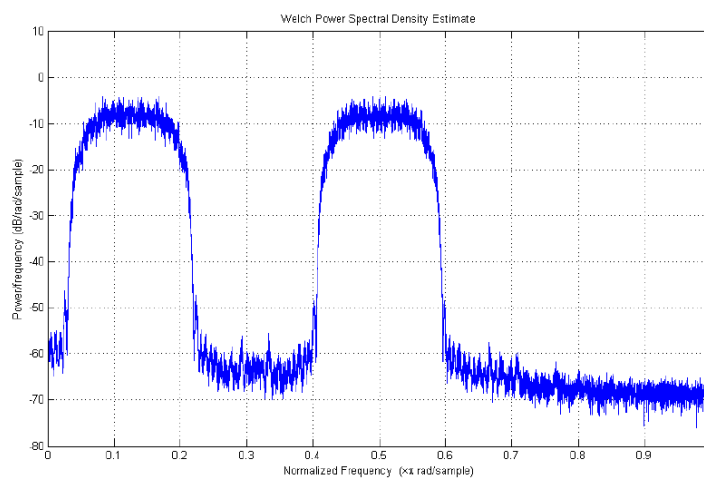


Figure 7. Test case 1 simulated.

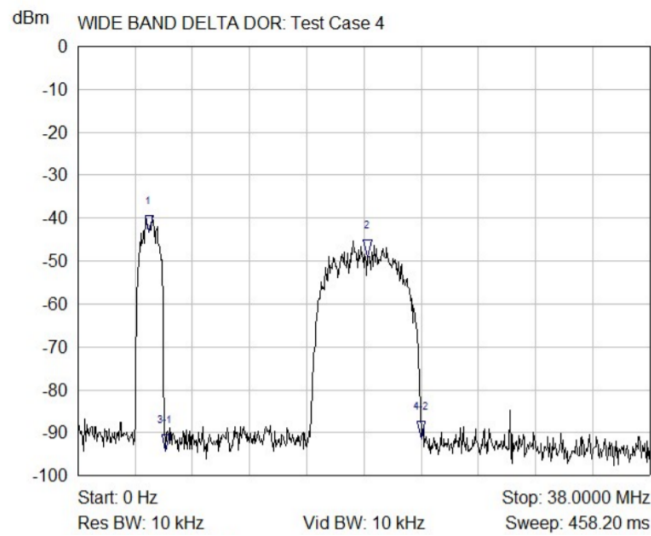


Figure 8. Test case 4 measured.

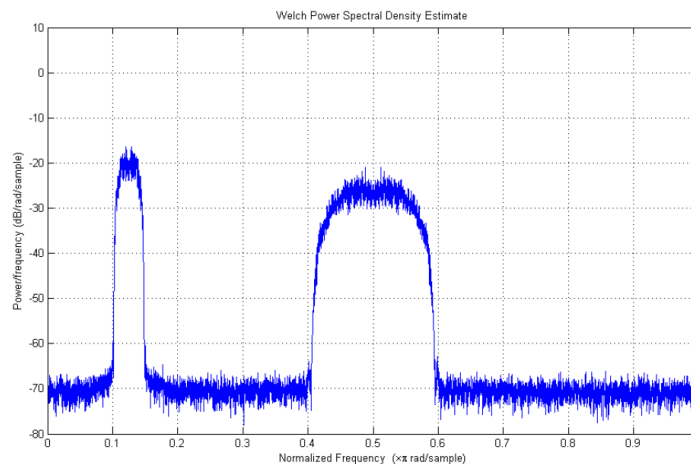


Figure 9. Test case 4 simulated.

#### 4. Conclusions

In this paper, the implementation of a Wideband  $\Delta$ DOR core for the tracking of interplanetary spacecraft is presented. It guarantees 1 nrad accuracy in ranging measurements. The algorithm was simulated in floating arithmetic to check the performances. A FLP to FXP optimization phase was performed to reduce the hardware complexity maintaining the specification of 50 dB of Dynamic Range on the generated RRC signal. The core was implemented in an ALTERA Stratix II EP2S180 FPGA. An experimental set up of the entire system based on an ALTERA Stratix II Development Board was implemented and measured. The proposed W- $\Delta$ DOR core will be used in the compatibility tests in the European Space Operations Centre (ESOC)—Darmstadt in Germany, to verify the accuracy performance of this technique. The next step will be the implementation of the W- $\Delta$ DOR core in radiation-hard FPGA technology to be featured in future interplanetary missions.

**Author Contributions:** Conceptualization, L.I. and G.C.C. and L.S.; methodology, D.G. and L.D.N. and R.F.; software, M.M. and D.G.; validation, M.M., and G.D.A. and F.C. and A.P.P.; formal analysis, L.I. and G.C.C. and L.S.; resources, L.S.; data curation, M.M.; writing—original draft preparation, M.R. and D.G. and M.M. and L.D.N. and R.F.; writing—review and editing, M.R. and M.M.; visualization, D.G. and M.M. and L.D.N. and R.F.; supervision, G.C.C. and L.S.; project administration, L.S.; funding acquisition, L.S.

**Funding:** This work was carried out in the frame of an ESA contract on “Flexible and Autonomous TT&C Transponders for Multi-Mission Applications” (Contract No. 4000114372/15/NL/FE).

**Conflicts of Interest:** The authors declare no conflict of interest.

## Abbreviations

The following abbreviations are used in this manuscript:

AMBA	Advanced Microcontroller Bus Architecture
CCSDS	Consultative Committee for Space Data Systems
CIC	Cascaded Integration Comb filter
$\Delta$ DOR	Delta-Differential One-Way Ranging
DDS	Direct Digital Synthesizer
FPGA	Field Programmable Gate Array
ESA	European Space Agency
ESOC	European Space Operations Centre
FLP	Floating Point
FXP	Fixed Point
LFSRs	Linear Feedback Shift Registers
PN	Pseudo Noise
RRCF	Root Raised Cosine Filter
SBI	Same Beam Interferometry
W- $\Delta$ DOR	Wideband $\Delta$ DOR

## References

- Iess, L.; Budnik, F.; Colamarino, C.; Corbelli, A.; Di Benedetto, M.; Fabbri, V.; Graziani, A.; Hunt, R.; James, N.; Lanucara, M.; et al. IDE-ONE: Improving Tracking Systems for Deep Space Navigation. In Proceedings of the 6th ESA International Workshop on Tracking, Telemetry and Command Systems for Space Applications, Darmstadt, German, 10–13 September 2013.
- Iess, L.; Mercolino, M.; Ardito, A.; Barboglio, F.; Jame, N. *Improvement of Delta-DOR Performances for One Nrad Accuracy for Precise Landing Support*; Technical Report; ESA; University of Rome “La Sapienza” and Thales Alenia Space: Rome, Italy, 2016.
- Lanyi, G.; Bagri, D.S.; Border, J.S. Angular Position Determination of Spacecraft by Radio Interferometry. *Proc. IEEE* **2007**, *95*, 2193–2201. [[CrossRef](#)]
- Border, J.S.; Koukos, J.A. Technical Characteristics and Accuracy Capabilities of Delta Differential One-Way Ranging (DeltaDOR) as a Spacecraft Navigation Tool. In Proceedings of the RF and Modulation Subpanel 1E Meeting at the German Space Operations Centre, Darmstadt, Germany, 20–24 September 1993.
- Andrei, A.; Souchay, J.; Zacharias, N.; Smart, R.; Martins, R.V.; da Silva Neto, D.; Camargo, J.; Assafin, M.; Barache, C.; Bouquillon, S.; et al. The Large Quasar Reference Frame (LQRF)-an optical representation of the ICRS. *Astron. Astrophys.* **2009**, *505*, 385–404. [[CrossRef](#)]
- Curkendall, D.W.; Border, J.S. Delta-DOR: The one-nanoradian navigation measurement system of the deep space network—History, architecture, and componentry. *Interplanet. Netw. Prog. Rep.* **2013**, *42*, 193.
- Madde, R.; Morley, T.; Lanucara, M.; Abello, R.; Mercolino, M.; De Vicente, J.; Sessler, G.M. A common receiver architecture for ESA radio science and delta-DOR support. *Proc. IEEE* **2007**, *95*, 2215–2223. [[CrossRef](#)]
- Thornton, C.L.; Border, J.S. *Radiometric Tracking Techniques for Deep-Space Navigation*; John Wiley & Sons: Hoboken, NJ, USA, 2005.
- Mercolino, M.; Ardito, A.; Barboglio, F.; Iess, N.J.; Mariani, M.J.; Racioppa, P.; Simone, L. A 1 nrad Delta-DOR System. In Proceedings of the TTC 2016, 7th ESA International Workshop on Tracking, Telemetry and Command Systems for Space Applications ESA-ESTEC, Noordwijk, The Netherlands, 13–16 September 2016.
- Iess, L.; Di Benedetto, M.; James, N.; Mercolino, M.; Simone, L.; Tortora, P. Astra: Interdisciplinary study on enhancement of the end-to-end accuracy for spacecraft tracking techniques. *Acta Astronaut.* **2014**, *94*, 699–707. [[CrossRef](#)]

11. Simone, L.; Gelfusa, D.; Ciarcia, S.; Fittipaldi, G. BepiColombo Ka-band transponder architectural design and performance analysis. In Proceedings of the TTC 2010, 5th ESA International Workshop on Tracking, Telemetry and Command Systems for Space Applications ESA-ESTEC, Noordwijk, The Netherlands, 21–23 September 2010.
12. Simone, L.; Gelfusa, D.; Ciarcia, S.; Fittipaldi, G. On-Board TTC Transponder for Secure Communications. In Proceedings of the MILCOM Military Communications Conference, Baltimore, MD, USA, 7–10 November 2011; pp. 1754–1759.
13. ESA. LEON2FT Microprocessor. 2017. Available online: [https://www.esa.int/Our\\_Activities/Space\\_Engineering\\_Technology/Microelectronics/LEON2-FT](https://www.esa.int/Our_Activities/Space_Engineering_Technology/Microelectronics/LEON2-FT) (accessed on 14 September 2017).
14. Hogenauer, E. An economical class of digital filters for decimation and interpolation. *IEEE Trans. Acoust. Speech Signal Process.* **1981**, *29*, 155–162. [[CrossRef](#)]
15. Ciarcia, S.; Simone, L.; Gelfusa, D.; Colucci, P.; De Angelis, G.; Argentieri, F.; Iess, L.; Formaro, R. MORE and Juno Ka-band transponder design, performance, qualification and in-flight validation. In Proceedings of the TTC 2013, 6th ESA International Workshop on Tracking, Telemetry and Command Systems for Space Applications ESA-ESTEC, Darmstadt, Germany, 10–13 September 2013.



© 2019 by the authors. Licensee MDPI, Basel, Switzerland. This article is an open access article distributed under the terms and conditions of the Creative Commons Attribution (CC BY) license (<http://creativecommons.org/licenses/by/4.0/>).